PHILOSOPHICAL TRANSACTIONS OF THE ROYAL SOCIETY A MATHEMATICAL, PHYSICAL & ENGINEERING SCIENCES

The Numerical Solution of the Differential Equations Governing the Reflexion of Long Radio Waves from the Ionosphere. II

K. G. Budden

Phil. Trans. R. Soc. Lond. A 1955 **248**, 45-72
doi: 10.1098/rsta.1955.0009

THE NUMERICAL SOLUTION OF THE DIFFERENTIAL EQUATIONS GOVERNING THE REFLEXION OF LONG RADIO WAVES FROM THE IONOSPHERE. II

By K. G. BUDDEN

Cavendish Laboratory, University of Cambridge

(*Communicated by J. A. Ratcliffe, F.R.S.—Received 25 October 1954*)

CONTENTS

This paper presents a series of curves which are the results of some calculations of the reflecting properties of various models of the ionosphere for radio waves of frequency 16 kc/s. The method of calculation was described in a previous paper (Budden 1955). No attempt is made to deduce a model of the ionosphere capable of explaining all the observations, but the aim has been rather to establish some general principles which may indicate how future theoretical and experimental work should be planned. In most of the calculations it was assumed that the earth's magnetic field is vertical and that the electron collision frequency in the ionosphere is constant. The limitations imposed by these restrictions are discussed.

The first half of the paper describes some calculations for a model of the ionosphere in which the electron density increases exponentially with height, and the second half deals with a model having both D- and E-layers. The results in both cases are compared with observations.

Vol. 248. A. 939. (Price 8*s.* 6*d.*) 7 [Published 12 May 1955

1. Introduction

Many experimental data are now available on the reflexion of long and very long radio waves from the ionosphere (see, for example, Bracewell, Budden, Ratcliffe, Straker & Weekes 1951). It is desirable to make the best possible use of these data to find out properties of the ionosphere, and in particular how the electron density and collision frequency vary with height. Unfortunately, there is no known way in which the experimental data may be used to deduce these properties directly. The best method of attack available at present is to make some plausible assumptions about how the electron density and collision frequency vary with height in the ionosphere, and to calculate the reflecting properties of this model ionosphere for long and very long waves. This is repeated for a series of models, and those models are selected which have properties most closely resembling the experimental results.

A program of work of this kind has been in progress for some time, using the EDSAC, the automatic digital computer in the University Mathematical Laboratory, Cambridge. The mathematical basis of the numerical methods used has been given in a previous paper (Budden 1955), hereinafter referred to as paper I. The purpose of the present paper is to give some of the results that have been obtained, and to compare them with the observations. No attempt is made to deduce a model of the ionosphere capable of explaining the observations. The aim has been rather to establish some general principles which may be of use in indicating how future theoretical and experimental work should be planned. The results are presented as a series of curves which apply to a frequency of 16 kc/s. Calculations are now in progress for higher frequencies, but have not proceeded far enough to allow the results to be included in this paper.

In paper I, two different numerical methods were described, and the results given in the present paper were obtained almost entirely by the first of these methods, an outline of which is given in §3. Most of the calculations were made for a vertical superimposed magnetic field and a fixed value of the electron-collision frequency. The limitations imposed by these restrictions are discussed in §4. Section 5 describes some calculations made for a model of the ionosphere in which the electron density increases exponentially with height, and the results of these calculations are discussed in §6. Section 7 is concerned with the properties of a model ionosphere with both *D*- and *E*-layers.

2. Notation

The notation is practically the same as in paper I. Electric and magnetic quantities are in rationalized units. Some of the more important symbols are as follows:

z	height measured vertically upwards
p	$2\pi \times$ frequency of waves
c	velocity of electromagnetic waves in free space
k	$p/c = 2\pi/\lambda$ (where λ is the wave-length in free space)
B	earth's magnetic induction
e, m	charge and mass of the electron
ϵ_0	electric permittivity of free space
N	electron density

ν collision frequency of electrons
X $Ne^2/\epsilon_0 mp^2$
Y eB/mp
Z ν/p
θ angle between the vertical and the wave normal of the incident wave below the ionosphere
C $\cos\theta$

${}_{\parallel}R_{\parallel}$, ${}_{\parallel}R_{\perp}$, ${}_{\perp}R_{\parallel}$, ${}_{\perp}R_{\perp}$ components of the reflexion coefficient, defined in §3

All field quantities in the electromagnetic waves are assumed to vary with time, t, through a factor e^{ipt}.

3. Outline of method of calculation

In discussing the return of plane waves from the ionosphere at oblique incidence, it is convenient to describe the incident and reflected waves in terms of their component electric fields parallel to, and perpendicular to, the plane of propagation, and to use the four symbols, ${}_{\parallel}R_{\parallel}$, ${}_{\parallel}R_{\perp}$, ${}_{\perp}R_{\parallel}$, ${}_{\perp}R_{\perp}$, for the (complex) ratio of a specified electric field in the wave after reflexion to a specified electric field in the wave before reflexion. The first subscript denotes whether the electric field of the incident wave is parallel ($_{\parallel}$) or perpendicular ($_{\perp}$) to the plane of incidence, and the second subscript refers in the same way to the electric field in the reflected wave.

To find these four quantities, the differential equations governing the variation with height of the four horizontal components E_x, E_y, $\mathscr{H}_x$, $\mathscr{H}_y$, of the total electromagnetic field of the wave were formulated, and solved by a step-by-step integration process proceeding downwards through the ionosphere. Each integration was started at a point high in the ionosphere using a specially chosen 'initial solution' satisfying the physical conditions. These conditions arise because the only influx of energy is in the incident wave below the ionosphere. At a high enough level the solution must therefore represent an upgoing wave. The differential equations are equivalent to a single fourth-order equation which has four independent solutions. At a sufficiently high level two of these are upgoing waves and two are downgoing waves. Thus there are two independent 'initial solutions' which satisfy the physical conditions at a high level, and therefore two integrations were performed, starting with these two solutions. These resulted in two independent sets of values of E_x, E_y, $\mathscr{H}_x$, $\mathscr{H}_y$ for a point below the ionosphere. Each set was separated into its component upgoing and downgoing waves which were in general elliptically polarized. The two sets were then combined to give the four quantities ${}_{\parallel}R_{\parallel}$, ${}_{\parallel}R_{\perp}$, ${}_{\perp}R_{\parallel}$, ${}_{\perp}R_{\perp}$.

The differential equations contain coefficients which are functions of the height z, and of the angle of incidence θ. The functional dependence on height arises through the quantities X and Z which are proportional respectively to the electron density and collision frequency. Most of the solutions described in the present paper are for models of the ionosphere in which X increases indefinitely with height, and the integrations were started at a level where X was very large, usually of the order of 10^3 to 10^4. The effect of this was to make the 'initial solutions' practically independent of the angle of incidence, so that, for any one model of the ionosphere, the same initial solutions could be used for all angles of incidence.

PHILOSOPHICAL TRANSACTIONS OF THE ROYAL SOCIETY A MATHEMATICAL, PHYSICAL & ENGINEERING SCIENCES

When X is very large, so that $X \gg Z$, the magneto-ionic medium can be treated as 'slowly varying', and the propagation of waves in it is then characterized by two refractive indices given by the Appleton–Hartree formula (Appleton 1932), which reduces to

$$\mu^2 \doteqdot \pm X/nY, \tag{1}$$

where n is the cosine of the angle between the earth's magnetic field and the vertical. One refractive index is therefore almost purely real and the other almost purely imaginary. Hence it may be inferred that one initial solution represents an upgoing progressive wave (μ almost purely real) and the other represents an evanescent wave (μ almost purely

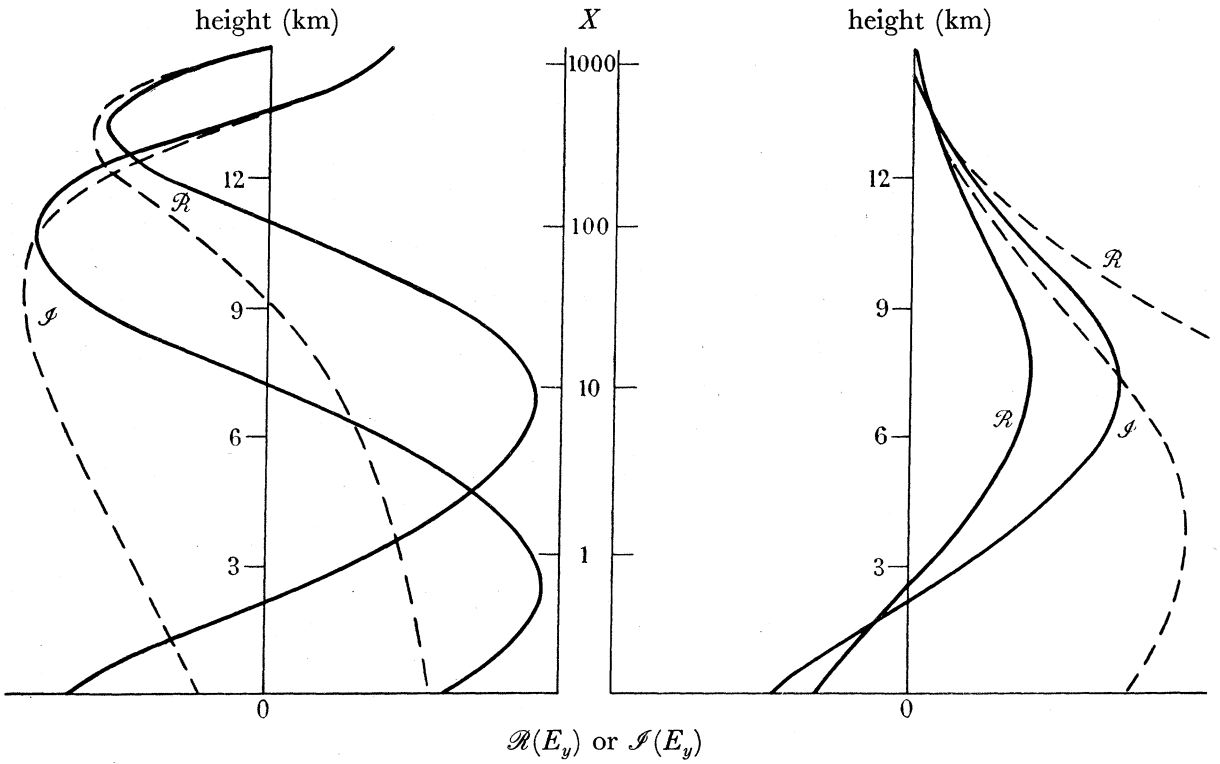

(*a*) nearly progressive wave solution. Angle of incidence: —, 0°; – – –, 83°.

(*b*) nearly evanescent wave solution. Angle of incidence: —, 0°; – – –, 55½°.

FIGURE 1. Variation of transverse electric field (real part, $\mathscr{R}$, and imaginary part, $\mathscr{I}$) with height, z, for a typical wave solution. $X = e^{\alpha z}$, where $\alpha = 0{\cdot}59$ km^{-1}, $Z = 8$.

imaginary). That this is so is shown in figure 1 (*a*) and (*b*), in which the real and imaginary parts of E_y are plotted as functions of height for the two solutions in a model ionosphere in which Z is constant and X increases exponentially with increasing height. Figure 1 (*a*) shows an example in which the real and imaginary parts of E_y varied roughly sinusoidally and were in quadrature. Hence E_y must be given approximately by: $E_y = \exp\{-if_1(z)\}$, where the function $f_1(z)$ has only a small imaginary part, and the solution therefore represents an upgoing progressive wave. For this solution μ was almost real. The figure also shows that the condition remained down to the lowest part of the ionosphere, so that the associated reflexion was very small. The other solution is illustrated in figure 1 (*b*), which shows that the real and imaginary parts of E_y are in a roughly constant ratio at all

levels, so that E_y must be given approximately by $E_y = A \exp\{-f_2(z)\}$ where the function $f_2(z)$ has only a small imaginary part, and A is a complex constant. For the upper part of the curves the field decreases rapidly as the height increases, so that the solution is practically an evanescent wave corresponding to the almost purely imaginary value of μ. In the lower part of the ionosphere both curves are oscillatory, so that the solution resembles a 'standing wave' and is associated with almost complete reflexion.

The data for figure 1 (a) and (b) were obtained by arranging that the EDSAC printed the values of the field components, including E_y, after each step of the integration. This was done in only a few cases while the working of the integration process was being checked. The time required for printing was considerable, and in most of the calculations this printing was omitted.

The values of ${}_{\parallel}R_{\parallel}$, ${}_{\parallel}R_{\perp}$, etc., were calculated for the level at which the integration was stopped. This was normally at a point below the ionosphere or at a low level within it, where the refractive indices were practically unity, and where $z = z_1$ say. If the integration had been continued to a still lower level, at $z = z_2$ say, the values of $|\,{}_{\parallel}R_{\parallel}\,|$, $|\,{}_{\parallel}R_{\perp}\,|$, etc., would clearly remain constant, but the values of arg ${}_{\parallel}R_{\parallel}$, arg ${}_{\parallel}R_{\perp}$, etc., would be decreased by $2k(z_1-z_2)\,C$ radians ($C = \cos\theta$), corresponding to the double transit of the distance z_1-z_2 at an angle θ to the vertical. Let arg ${}_{\parallel}R_{\parallel} = \phi$ for a general value of z, and let $\phi = \phi_1$ when $z = z_1$. Both ϕ and ϕ_1 are functions of the angle of incidence, θ, and therefore also of C. Then

$$\phi(C) = \phi_1(C) + 2kC(z-z_1). \tag{2}$$

It is clearly necessary to specify the level to which values of arg ${}_{\parallel}R_{\parallel}$, arg ${}_{\parallel}R_{\perp}$, etc., refer. This level need not necessarily be lower than the level where the integration was stopped. For models of the ionosphere in which X varied exponentially with height, it was convenient to take the level where $X = 1$ as the reference level. The integrations were always stopped at a level below this, and the corrections to arg ${}_{\parallel}R_{\parallel}$, etc., were made by adding $2k(z_0-z_1)\,C$ radians, where $X = 1$ at $z = z_0$. Where values of arg ${}_{\parallel}R_{\parallel}$ are displayed in the figures of this paper, the reference level is always specified.

It is in general possible to find a reference level such that, at least for a small range of values of C, the value of $\phi = \arg {}_{\parallel}R_{\parallel}$ is practically constant. This requires that

$$\frac{\mathrm{d}\phi}{\mathrm{d}C} = 0 = \frac{\mathrm{d}\phi_1}{\mathrm{d}C} + 2k(z-z_1). \tag{3}$$

The value of z which satisfies (3) is called, by Bracewell *et al.* (1951) the 'apparent' height of reflexion.

4. Effect of varying collision frequency and of obliquity of the earth's magnetic field

The problem of solving the differential equations is greatly simplified if it can be assumed that the earth's magnetic field is vertical, and that Z (proportional to collision frequency) is independent of height, and these assumptions were made in all the calculations described in later sections of this paper. It was, however, desirable to investigate whether they introduced any serious errors, and the present section describes some calculations made for this purpose.

(*a*) *Varying collision frequency*

A number of calculations were made in which it was assumed that the earth's magnetic field was vertical, that X increased exponentially with height z according to the law $X \propto e^{\alpha z}$, and that Z decreased exponentially with increasing height according to the law $Z \propto e^{-z/H}$, where z is in kilometres and $H = 10$ km. This is probably close to the actual law of variation of Z with height at the level where long and very long waves are reflected. Some typical results are shown in figure 2, in which $|\,{}_{\parallel}R_{\parallel}\,|$, $|\,{}_{\parallel}R_{\perp}\,|$ and $\arg\,{}_{\parallel}R_{\parallel}$ are plotted as functions of angle of incidence. The same figure also shows curves (dotted) calculated

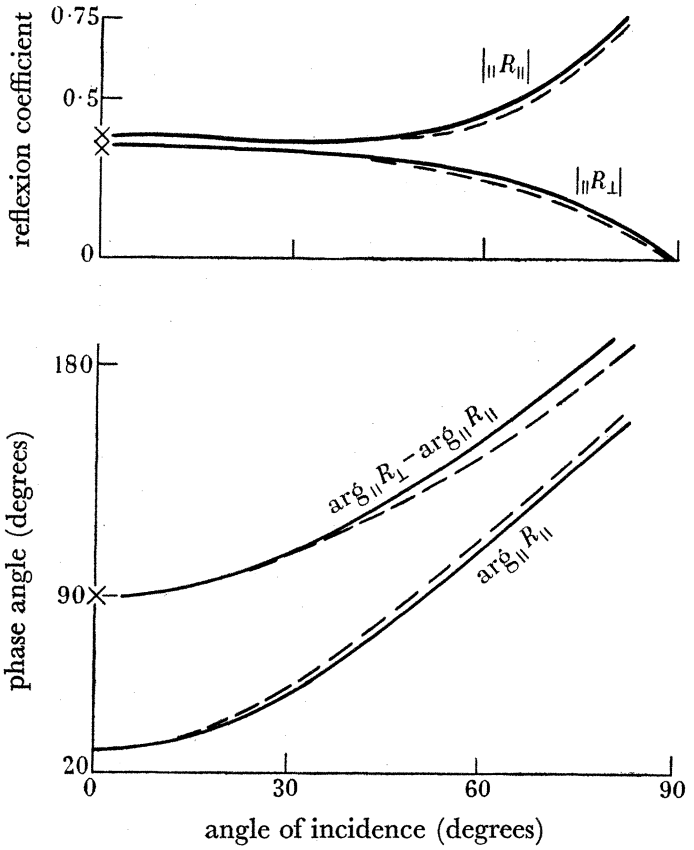

FIGURE 2. Comparison of results with Z varying and with Z fixed. For full curves, $Z \propto e^{-z/H}$, where $H = 10$ km. When $X = 80$ $(= Y)$, $Z = 17{\cdot}3$. For dashed curves $Z = 17{\cdot}5$ (fixed). For both curves $X = e^{\alpha z}$, where $\alpha = 0{\cdot}59$ km^{-1}. Values of $\arg\,{}_{\parallel}R_{\parallel}$ refer to the level where $X = 1$. Points marked thus $\times$ were calculated by the analytic method given in paper I, appendix 1.

for the same model ionosphere, except that Z was held constant at a value equal to the value of Z for the full curves at the level where $X = Y$. It is seen that the curves are practically indistinguishable. The same measure of agreement was obtained in all the calculations of this kind that were tried. It is well known that the level in the ionosphere where $X = Y$ is of great importance in reflecting long and very long waves (see, for example, Heading & Whipple (1952), who call this level 'region II').

The conclusion is that for models of the ionosphere in which the earth's magnetic field is vertical and X increases exponentially with height, it is permissible to treat Z as a constant equal to its true value at the level where $X = Y$.

(*b*) *Obliquity of the earth's magnetic field*

When the earth's magnetic field was oblique the differential equations became much more complicated and the programming of a calculation for the most general case was too long to be practicable. It was found, however, that by taking the angle between the earth's magnetic field and the vertical to be 30° and considering only (magnetic) east-

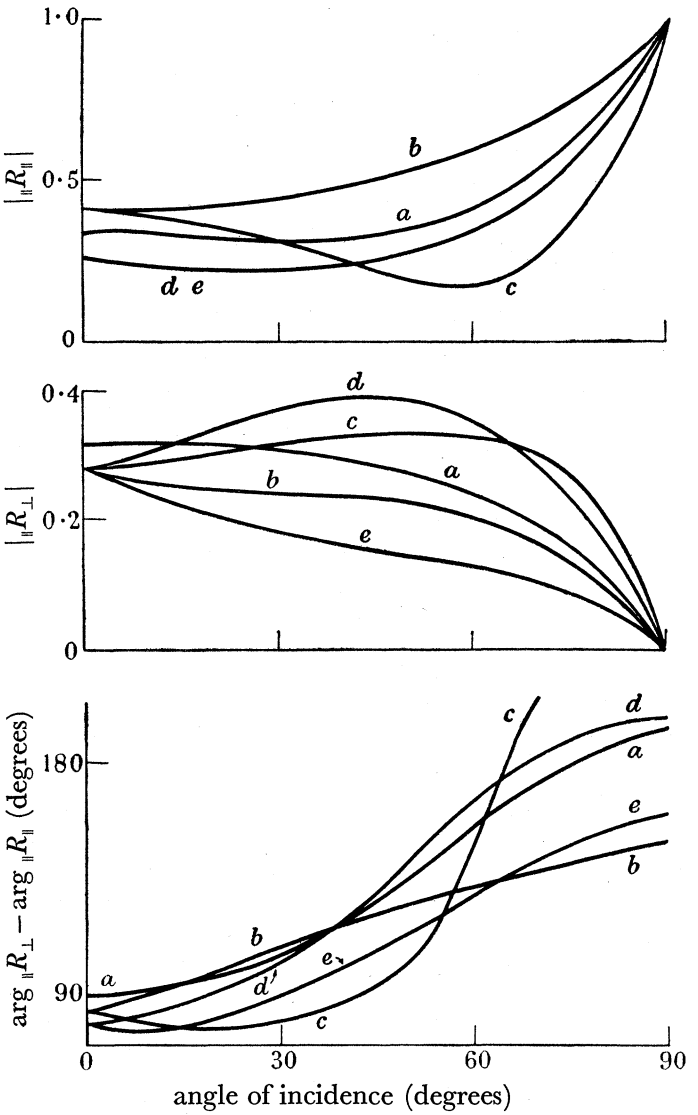

FIGURE 3. Comparison of results for vertical and oblique magnetic fields. For all curves $Z = 30$ (fixed), $X = e^{\alpha z}$, where $\alpha = 0{\cdot}59\ \mathrm{km}^{-1}$. For oblique field curves angle of magnetic dip = 60°. The curves are labelled as follows: (*a*) vertical magnetic field; (*b*) oblique field, propagation from (magnetic) east to west, (*c*) oblique field, propagation from (magnetic) west to east, (*d*) oblique field, propagation from (magnetic) north to south, (*e*) oblique field, propagation from (magnetic) south to north.

west and north-south propagation, the programs could be made short enough to use. Even so, the time for a calculation was very long, and only a few results have been obtained. The second method of calculation described in paper I promises to provide a much quicker method of making these calculations.

One set of results obtained with an oblique magnetic field was concerned with reciprocity for (magnetic) north-south and south-north propagation. These have been described elsewhere (Budden 1954).

Figure 3 is a comparison of some results for oblique and for vertical magnetic field. For all the curves Z was constant and X increased exponentially with height. It is clear that there are wide differences between the results calculated with oblique and vertical fields, and hence results obtained with a vertical magnetic field can only be regarded as giving a qualitative indication of the properties of the actual ionosphere at latitudes such as those in England, where many of the experimental results were obtained.

There seem to be very few observations with which results such as those of figure 3 can be compared. Tremellen (1950) has observed that for propagation over distances of the order of 6000 km, signals from very low-frequency transmitters to the west are received more strongly than from those to the east. The few calculations that have been done all show that $|{}_{\parallel}R_{\parallel}|$ is greater for propagation from east to west, which is opposite to Tremellen's result. However, for such large propagation distances as 6000 km it is not practicable to regard the propagation in terms of a small number of single reflexions at the ionosphere. It would be more correct to treat the space between the earth and the ionosphere as a wave guide (see, for example, Budden 1953). The properties of this guide could be deduced from theoretical curves such as those of figure 3, but the calculation would be complicated, and a higher accuracy would be needed, for angles of incidence near grazing, than has so far been attained. Meanwhile it cannot be said that Tremellen's result conflicts with the theory.

5. Calculations with exponential increase of X, constant Z and vertical magnetic field

At the time when the calculations described in this paper were started, some progress had already been made with the numerical solution of the equations for a frequency of 150 kc/s, and vertical incidence (Gibbons & Nertney 1951), but comparatively little was known about the solutions for lower frequencies. Because of the extensive observations that have been made at a frequency of 16 kc/s (Bracewell *et al.* 1951) it was decided to investigate the solutions for this frequency first. The observations consisted largely of measurements of $|{}_{\parallel}R_{\parallel}|$, $\arg {}_{\parallel}R_{\parallel}$, $|{}_{\parallel}R_{\perp}|$, $\arg {}_{\parallel}R_{\perp} - \arg {}_{\parallel}R_{\parallel}$, and of their changes with time of day, season and during ionospheric disturbances. Some attempts have been made to explain the observations in terms of specific models of the ionosphere (for example, Bracewell & Bain 1952), and most of these postulate a subsidiary ionized region, called the D-layer, in the ionosphere at a height between 70 and 100 km. However, because of the uncertain theoretical knowledge of the reflecting properties of any model ionosphere at 16 kc/s it seemed important to investigate whether the results could be explained without postulating a D-layer. It was possible that the ionization in the lower part of the E-region might be adequate to explain the observed results, and the work of Heading & Whipple (1952) had indicated that under some conditions an ionosphere in which X increased monotonically with height could behave as though reflexion occurred simultaneously at two different levels.

The object of the first calculations was therefore to establish the general properties of a model ionosphere in which X increased monotonically with height. In a problem of this kind one possible law for the variation of X with height is that deduced by Chapman (1931), for the lower part of the ionized layer formed in an isothermal atmosphere by monochromatic radiation. It is, however, known that very long waves are reflected at a height

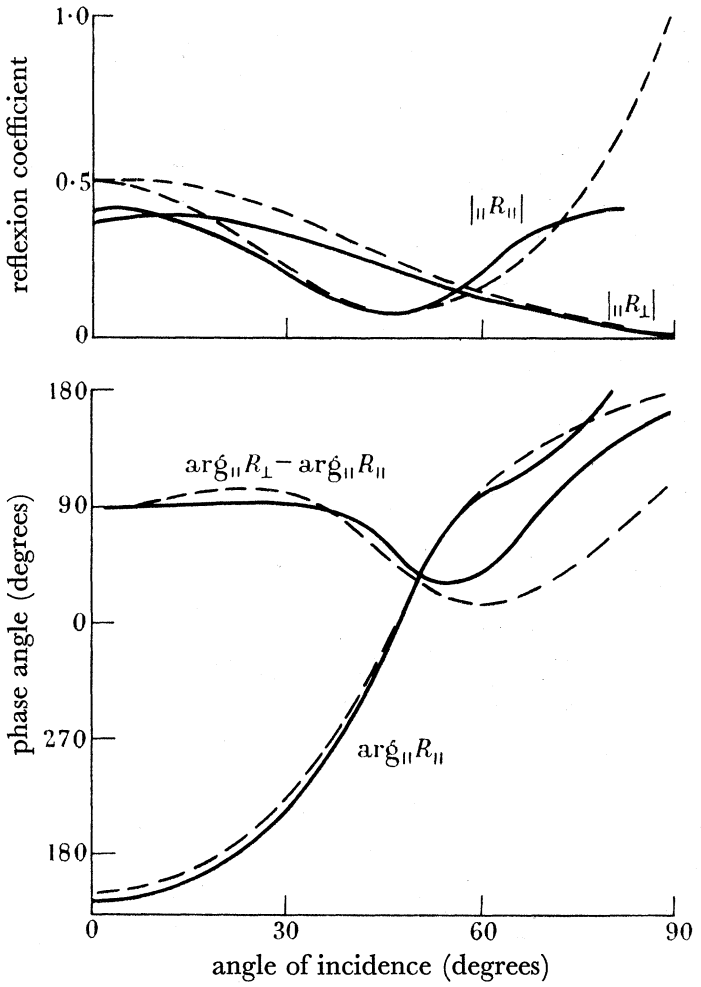

FIGURE 4

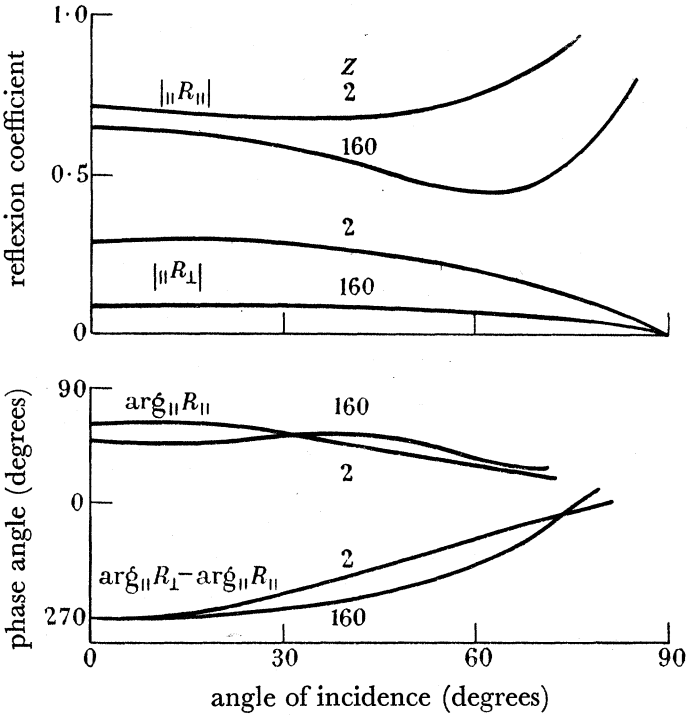

FIGURE 5

FIGURE 4. Comparison of numerical results with analytic solution. Full curves were calculated by EDSAC. Dashed curves used the formulae of Heading & Whipple. For all curves $Z = 8$, $X = e^{\alpha z}$, where $\alpha = 0{\cdot}295\ \mathrm{km}^{-1}$. Points marked $\times$ were calculated by the method of paper I, appendix 1. Values of arg $_{\parallel}R_{\parallel}$ refer to the level where $X = 1$.

FIGURE 5. Results for a 'sharp layer' and for very small and very large values of Z. $X = e^{\alpha z}$, where $\alpha = 2{\cdot}36\ \mathrm{km}^{-1}$. Values of arg $_{\parallel}R_{\parallel}$ refer to the level where $X = 1$.

of the order of 70 km in the daytime. If the E-layer of the ionosphere were a Chapman layer, the ionization in its lower part would fall off so quickly as the height decreased, that at a height of 70 km the ionization density would be much too small to reflect very long waves. This suggests that a law should be chosen in which, as the height decreases, the electron density decreases more slowly than in a Chapman layer. An exponential law has this property and was particularly convenient because the successive values of X were

easily calculated during the integration by multiplying the current value by a constant fraction. Moreover, in the first calculations the object was to compare the reflecting properties of a 'rapidly varying' or 'sharp' ionosphere and a 'slowly varying' or 'gradual' ionosphere. The law chosen was $X = e^{\alpha z}$, where α is a constant which is small for a

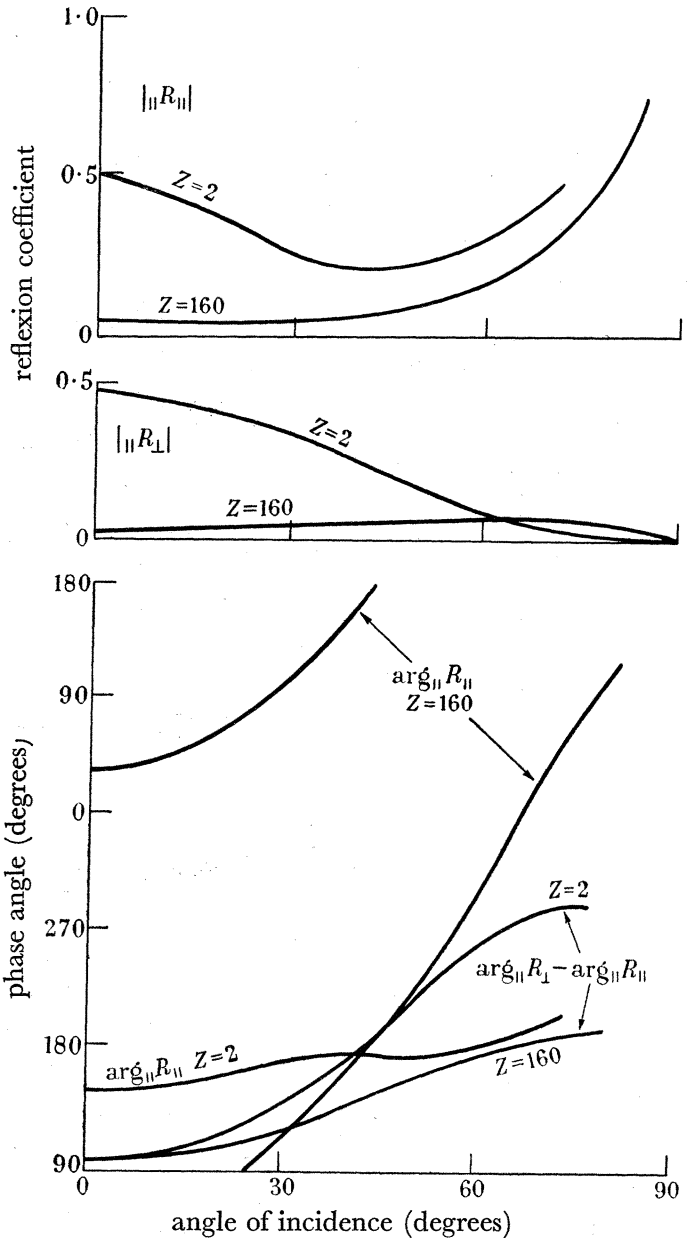

FIGURE 6. Results for a 'gradual layer' and for very small and very large values of Z. $X = e^{\alpha z}$, where $\alpha = 0{\cdot}295$ km^{-1}. Values of arg $_{\parallel}R_{\parallel}$ refer to the level where $X = 1$.

'gradual' ionosphere, and large for a 'sharp' ionosphere. Four different values of α were used, namely, 0·285, 0·59, 1·18 and 2·36 km^{-1}.

A second object was to study the effect of the collision frequency ν on the reflecting properties of the ionosphere. For reasons given in the last section ν, and therefore Z, were treated as constants in most of the calculations. For the frequency of 16 kc/s, the values

of Z used ranged from 2 to 320, corresponding to values of ν from 2×10^5 to $3{\cdot}2\times10^7\,\mathrm{s}^{-1}$. At a height of 80 km it appears probable (Nicolet 1953) that the true value of ν is about $3\times10^6\,\mathrm{s}^{-1}$, giving $Z=30$ at 16 kc/s.

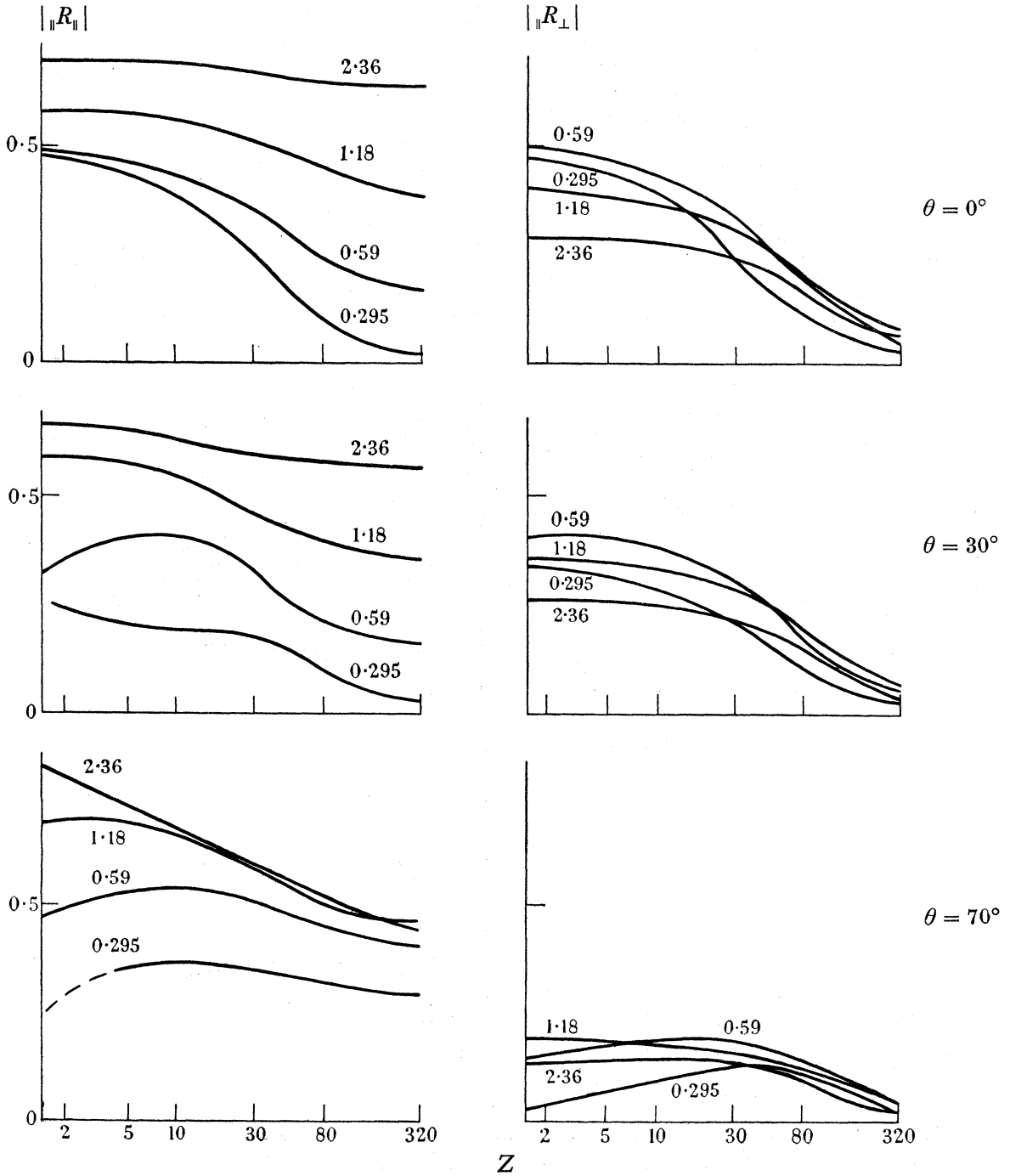

FIGURE 7. Variation of $|{}_{\parallel}R_{\parallel}|$ and $|{}_{\parallel}R_{\perp}|$ with Z (proportional to collision frequency). $X=\mathrm{e}^{\alpha z}$. Values of α given in km^{-1} on the curves.

The results were plotted in the form of curves showing the quantities $|{}_{\parallel}R_{\parallel}|$, $|{}_{\parallel}R_{\perp}|$, $\arg {}_{\parallel}R_{\parallel}$ and $\arg {}_{\parallel}R_{\perp} - \arg {}_{\parallel}R_{\parallel}$ as functions of the angle of incidence. Some curves are shown in figures 2 to 6. Figure 4 is for the small value $Z=8$, and is important because the

condition $Z \ll Y$ is fairly well fulfilled (for 16 kc/s, $Y = 80$), and it is possible to apply to this case the analytic solution of Heading & Whipple (1952). The results obtained from their formulae are shown as dashed curves in figure 4. Their method involves some

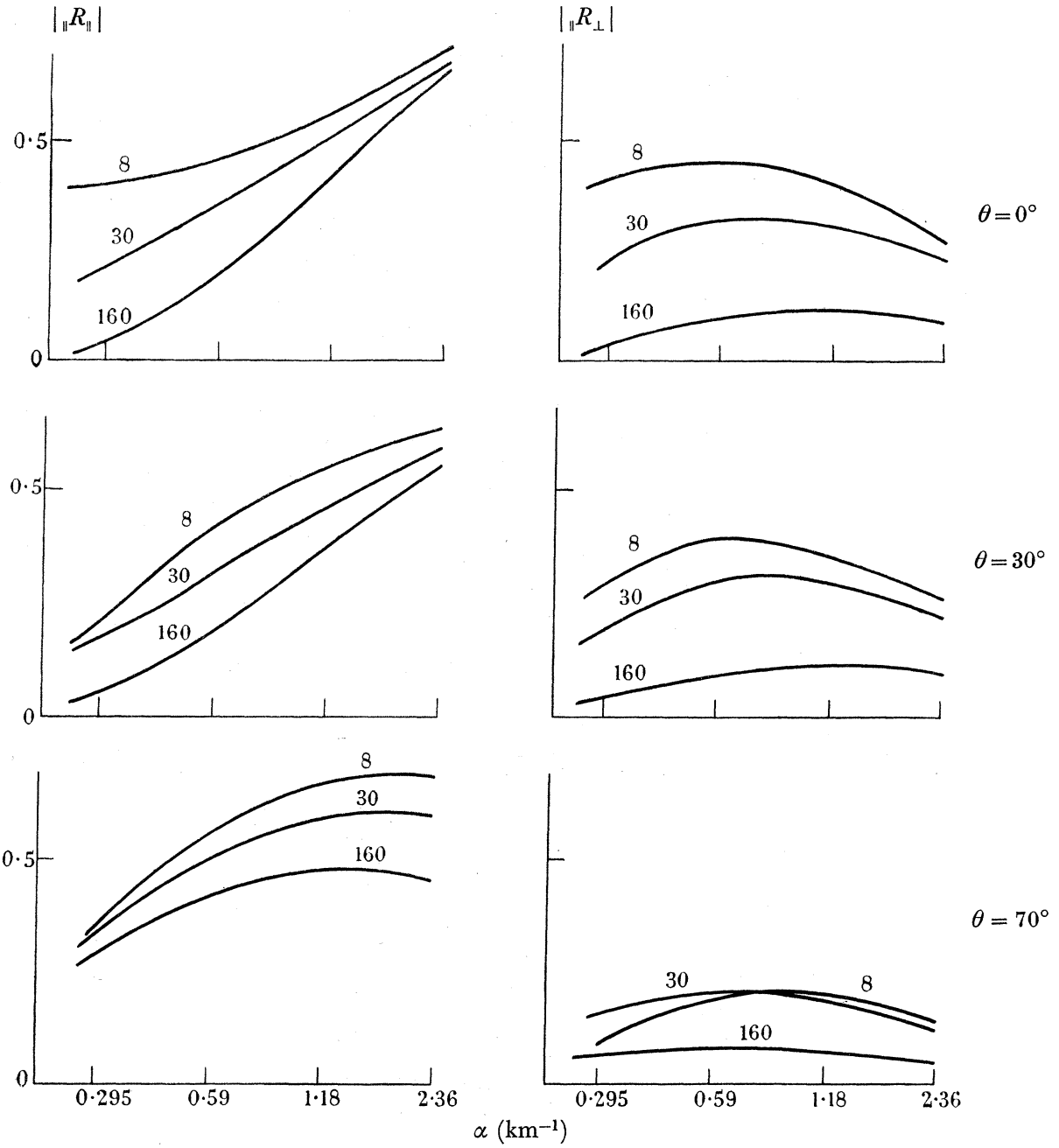

FIGURE 8. Variation of $|_{\parallel}R_{\parallel}|$ and $|_{\parallel}R_{\perp}|$ with α, where $X = e^{\alpha z}$, for various indicated values of Z (proportional to collision frequency).

approximation, so that exact agreement is not expected. The more marked disagreement for large angles of incidence is probably due to a rather abstruse source of error in the EDSAC programs, which was explained in appendix 2 of paper I.

Figures 5 and 6 are arranged to show the relative effects of very small and very large values of Z. Figure 5 is for a 'sharp' and figure 6 is for a 'gradual' ionosphere. In order

to display more clearly the effects of varying α and Z, some further sets of curves are shown in figures 7, 8 and 9. Each curve in figure 7 is plotted for a fixed angle of incidence and a fixed value of α and shows how $|\,{}_{\parallel}R_{\parallel}\,|$ or $|\,{}_{\parallel}R_{\perp}\,|$ varies with Z. Similarly in figure 8, each

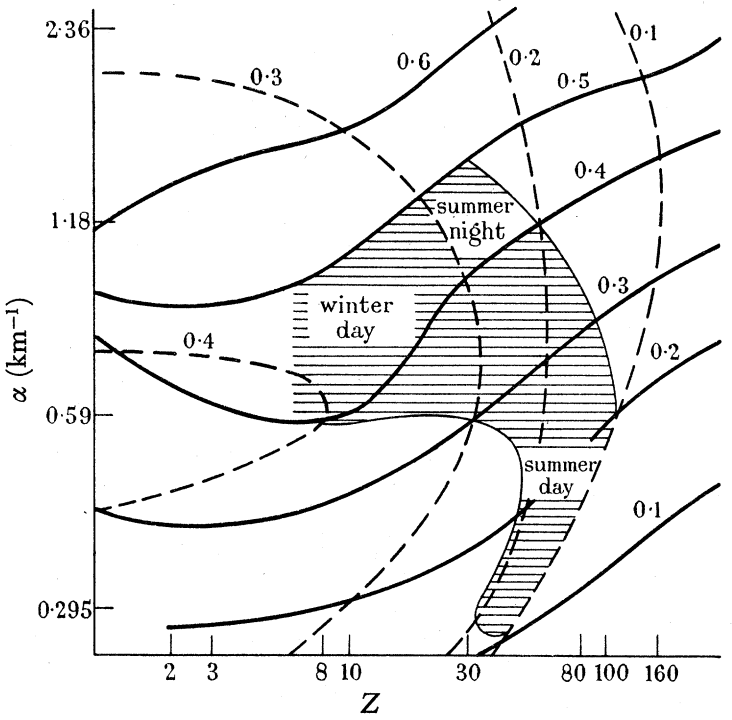

FIGURE 9. Contours in the $\alpha - Z$ plane, showing loci of points for which $|\,{}_{\parallel}R_{\parallel}\,|$ (full curves) and $|\,{}_{\parallel}R_{\perp}\,|$ (dashed curves) have specified constant values. $\theta = 30°$. Vertical magnetic field.

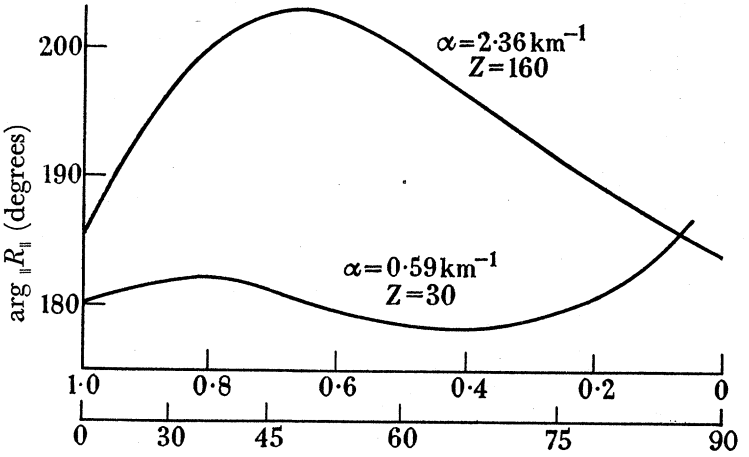

FIGURE 10. Variation of arg $_{\parallel}R_{\parallel}$ with $\cos\theta$. For both curves $X = e^{\alpha z}$. For the top curve values of arg $_{\parallel}R_{\parallel}$ refer to the level where $X = 0{\cdot}073$, and for the bottom curve they refer to the level where $X = 10$.

curve is for a fixed angle of incidence and a fixed value of Z, and shows how $|\,{}_{\parallel}R_{\parallel}\,|$ or $|\,{}_{\parallel}R_{\perp}\,|$ varies with α. Some of the same information is displayed in a different way in figure 9, which is for an angle of incidence of 30°. (This is roughly the value for waves received at Cambridge from the 16 kc/s transmitter GBR at Rugby, on which many

observations were made (Bracewell *et al.* 1951).) The ordinates are values of α, and the abscissae values of Z. In the resulting α-Z plane, contours are plotted of equal values of $|\,{}_{\parallel}R_{\parallel}\,|$ and $|\,{}_{\parallel}R_{\perp}|$. The significance of the shaded area in this figure is explained in §6 (*c*). In figure 10 arg ${}_{\parallel}R_{\parallel}$ is plotted against cos θ for two cases. The value of this type of curve will be evident in §6 (*a*).

6. Discussion of results for 'exponential' ionosphere

It is now of interest to ask what features of the properties of the 'exponential' models of the ionosphere discussed in the last section can be correlated with the experimental results. It is convenient to discuss this correlation under some of the same main headings as those used by Bracewell *et al.* (1951).

(*a*) '*Apparent*' *height of reflexion*

Although radio waves are probably returned to the earth by some process of gradual deviation, it is convenient to discuss the results as though reflexion occurred from a mirror-like surface, which is imagined to be at such a level that no change of phase occurs when the angle of incidence is varied. The height of this fictitious surface is called the 'apparent' height of reflexion, and a formal definition is given in §3 (equation (3)). Weekes (1950), using Hollingworth's method of the interference pattern, has shown that with waves of frequency 16 kc/s observed during a summer day, a winter day, and a summer night, the results can be represented by a simple model with such a horizontal fictitious reflecting surface for angles of incidence up to about 65°. For greater angles of incidence, some rather fundamental change appears to occur in the reflexion phenomena.

To test whether this result would occur with an 'exponential' ionosphere, it is convenient to plot arg ${}_{\parallel}R_{\parallel}$ against $C = \cos\theta$, as has been done in figure 10 for two typical cases. Any part of the resulting curve which is straight indicates that there is a fixed apparent height of reflexion for the corresponding range of values of C or θ. Thus, for the case $\alpha = 2{\cdot}36$ km^{-1}, $Z = 160$ illustrated in figure 10, there is a nearly constant apparent height for the approximate range $0 \leqslant \theta \leqslant 35°$, and another nearly constant apparent height, about 2·9 km lower, for the range $55° \leqslant \theta \leqslant 90°$. Similarly for the other curve, for which $\alpha = 0{\cdot}59$ km^{-1}, $Z = 30$, the apparent height is lower for the range $40° \leqslant \theta \leqslant 65°$ than for the range $0° \leqslant \theta \leqslant 25°$.

It is interesting to compare the curves of figure 10 with the corresponding curves for $|\,{}_{\parallel}R_{\parallel}\,|$. These are shown in figure 5 and figure 3 respectively. The curve for $\alpha = 2{\cdot}36$ km^{-1}, $Z = 160$ in figure 5 is seen to have a distinct minimum. It was found that in nearly all cases where such a minimum occurred in the curve for $|\,{}_{\parallel}R_{\parallel}\,|$, there was an associated change of slope in the curve of arg ${}_{\parallel}R_{\parallel}$ against C. For the other case ($\alpha = 0{\cdot}59$ km^{-1}, $Z = 30$, 'vertical field' curve in figure 3), the minimum is much less pronounced, and the lower curve in figure 10 correspondingly shows a smaller change of slope.

Properties similar to the above are displayed by the reflexion coefficient of a sharply bounded homogeneous medium. Curves of such reflexion coefficients have been given by Pedersen (1927) for isotropic media, and by Budden (1951) for ionized media with a superimposed magnetic field. Many of the curves of $|\,{}_{\parallel}R_{\parallel}\,|$ against θ in both these cases show a minimum at an angle θ which has been called the 'quasi-Brewster' angle, and

there is an associated change in curves of arg $_{\parallel}R_{\parallel}$ against θ which is most pronounced in those cases where the minimum is most marked. For the 'exponential' ionosphere, the minima and their associated phase changes are most apparent when the ionosphere is 'sharp' (high values of α), and it is convenient to speak of the 'quasi-Brewster' angle in this case also. It is possible that the discontinuity in reflexion conditions near $\theta = 65°$ observed by Weekes is connected in some way with a 'quasi-Brewster' angle phenomenon. The exponential ionosphere would provide a partial explanation of this, but it gives too low a value for the 'quasi-Brewster' angle (45 to 50° instead of 65°), and the high value of α required (almost 2·36 km^{-1}) must be excluded for other reasons (see §§ 6 (*b*) and (*d*)).

It is of interest to ask what is the value of X at the apparent height of reflexion in an exponential ionosphere. The calculated values for angles of incidence near vertical are shown in table 1. The table shows that for a 'gradual' ionosphere ($\alpha = 0{\cdot}295$ km^{-1}) the apparent height of reflexion may approach the level where $X = Y$ (at 16 kc/s, $Y = 80$), whereas for a 'sharp' ionosphere ($\alpha = 2{\cdot}36$ km^{-1}) the 'reflexion' occurs where the values of X are much smaller, and this may be associated with the much steeper vertical gradient of electron density.

TABLE 1. APPROXIMATE VALUES OF X AT 'APPARENT' HEIGHT OF REFLEXION, FOR ANGLES OF INCIDENCE NEAR VERTICAL. THE CORRESPONDING VALUES OF THE ELECTRON DENSITY, N, IN CM^{-3}, ARE SHOWN IN BRACKETS

α (km^{-1}) \ Z	2	8	30	80	160
0·295	26 (91)	52 (183)	72 (253)	72 (253)	72 (253)
0·59	78 (274)	21 (74)	11 (39)	13 (46)	21 (74)
1·18	1·6 (5·6)	1·6 (5·6)	1·6 (5·6)	3·8 (13)	3·5 (12)
2·36	0·01 (0·035)	0·07 (0·25)	0·33 (1·2)	1·3 (4·6)	10 (35)

(*b*) *Polarization of the reflected wave*

Observations of the reflected wave for a frequency of 16 kc/s, and for angles of incidence from 0 to about 50°, show that it is approximately circularly polarized with an anticlockwise rotation when viewed along the direction of propagation (left-handed rotation) (Best, Ratcliffe & Wilkes 1936; Budden, Ratcliffe & Wilkes 1939). For angles of incidence greater than about 65° it is approximately linearly polarized with the plane of polarization rotated through a small angle from the vertical plane. (Bracewell *et al.* (1951) state that the rotation is through 45° in a clockwise sense, but this is now believed to be incorrect, and there is some doubt as to how the observations should be interpreted.) These results imply that:

(i) for $0 \leqslant \theta \leqslant 50°$, $|\,{}_{\parallel}R_{\parallel}\,| \doteqdot |\,{}_{\parallel}R_{\perp}\,|$;
(ii) for $0 \leqslant \theta \leqslant 50°$, $\arg {}_{\parallel}R_{\perp} - \arg {}_{\parallel}R_{\parallel} \doteqdot 90°$;
(iii) for $60° \leqslant \theta \leqslant 80°$, $\arg {}_{\parallel}R_{\perp} - \arg {}_{\parallel}R_{\parallel} \doteqdot 0°$ or 180°.

For an 'exponential' ionosphere and vertical incidence there is an analytic solution (paper I, appendix 1), which shows that when $Y \gg 1$, $\arg {}_{\parallel}R_{\perp} - \arg {}_{\parallel}R_{\parallel} = 90°$. (For a frequency of 16 kc/s, $Y = 80$.) This result is confirmed by all the theoretical curves (including figures 2 to 6), which show also that the value increases as θ increases, and in

most cases approaches 180° when θ is nearly 90°, in fair agreement with the observed results (ii) and (iii). The calculated values of the ratio $|\,{}_{\parallel}R_{\perp}\,|/|\,{}_{\parallel}R_{\parallel}\,|$ were found to depend fairly markedly on the value of α, and to be much less dependent on the value of Z. For $\theta<60°$, and for $\alpha = 0{\cdot}295$, $0{\cdot}59$ and $1{\cdot}18$ km^{-1}, most of the values were between $0{\cdot}5$ and $1{\cdot}5$. For $\alpha = 2{\cdot}36$ km^{-1}, however, the ratio was smaller, as is shown in figures 5 and 7. This value of α would therefore be excluded by the observed result (i). For greater values of θ ($>60°$), the calculated value of $|\,{}_{\parallel}R_{\perp}\,|/|\,{}_{\parallel}R_{\parallel}\,|$ nearly always fell below $0{\cdot}5$.

(*c*) *Amplitude of the reflected wave*

Probably the most reliable measurements of $|\,{}_{\parallel}R_{\parallel}\,|$ were those made by Hollingsworth's method of the interference pattern. At 16 kc/s the observed values of $|\,{}_{\parallel}R_{\parallel}\,|$ obtained by this method and given by Weekes (1950) for small angles of incidence, were as follows: for a summer day $0{\cdot}14$; for a winter day $0{\cdot}27$; and for a summer night $0{\cdot}35$.*

In most of the other measurements of the amplitude of the reflected wave for nearly vertical incidence at 16 kc/s the value of $|\,{}_{\parallel}R_{\perp}\,|$ was measured, but since experiments have shown that the wave is approximately circularly polarized, it may be assumed that $|\,{}_{\parallel}R_{\perp}\,|/|\,{}_{\parallel}R_{\parallel}\,|$ is between $\frac{1}{2}$ and 1. The main series of measurements was for the sender GBR, received at Cambridge, for which the angle of incidence was about 30°. The diagram of figure 9 is plotted for this angle, and is useful in an attempt to correlate the observations with the properties of an 'exponential' ionosphere. Each point in this diagram represents a particular model ionosphere, and an attempt will be made to find the point corresponding to the model which best represents the observations.

The observed values of $|\,{}_{\parallel}R_{\perp}\,|$ varied with the time of day and time of year, but were roughly as follows: for a summer day $0{\cdot}1$; for a summer night $0{\cdot}25$; for a winter day $0{\cdot}35$; and for a winter night $0{\cdot}55$. The last value is greater than any of the values calculated for an exponential ionosphere, and the dashed curves of figure 9 suggest that it could only be achieved with an unreasonably small value of Z. If this large value is disregarded, then the observations suggest that the required representative point is within the shaded region in figure 9 which is bounded by the lines $|\,{}_{\parallel}R_{\parallel}\,| = 0{\cdot}5$ and $|\,{}_{\parallel}R_{\perp}\,| = 0{\cdot}1$ (greatest and smallest values, respectively), $|\,{}_{\parallel}R_{\perp}\,|/|\,{}_{\parallel}R_{\parallel}\,| = \frac{1}{2}$ and 1, and on the left by the line $Z = 8$. This last value corresponds to a collision frequency ν equal to 8×10^5 s^{-1}, which is about the smallest value that could be accepted for levels below about 90 km (Nicolet 1953).

The representative point for a summer day would be somewhere in the lower right-hand part of the shaded region; for a winter day it would be to the left and for a summer night in the upper right-hand part of the region. This arrangement is, however, unsatisfactory in several other respects. It would indicate that the effective value of Z is greater in a summer night than in a winter day, in conflict with observations of the apparent height of reflexion (Bracewell *et al.* 1951), which is about 13 km lower in a winter day than in a summer night, and would mean that the winter day value of Z should be the larger by a factor of 2 to 3. It would indicate that the ionosphere in summer is 'sharper' at night than by day, whereas it might be expected to become more 'gradual' at night when the sun's ionizing radiation is removed.

* Private communication from Dr Weekes.

PHILOSOPHICAL TRANSACTIONS OF THE ROYAL SOCIETY A MATHEMATICAL, PHYSICAL & ENGINEERING SCIENCES

(*d*) *Diurnal and seasonal changes; effects of sudden ionospheric disturbances*

One of the striking features of the observations at 16 kc/s for nearly vertical incidence is that on any one day between about 1 h after sunrise and 1 h before sunset, the value of $_{\parallel}R_{\perp}$ remains practically constant. This applies both in summer and in winter. During this time, the apparent height of reflexion varies through a range of about 13 km in winter and 17 km in summer. These large changes of height must almost certainly be associated with changes of collision frequency, and therefore of Z by a factor of the order of 2 to 4. Figure 9 shows that with an exponential model such a large change of Z would certainly give a detectable change in $|\,_{\parallel}R_{\perp}\,|$. The absence of such a change is a strong indication that the exponential model is inadequate to explain the observations.

A similar objection results from observations during sudden ionospheric disturbances. It is then found that $|\,_{\parallel}R_{\perp}\,|$ remains practically constant, whereas the apparent height may decrease by as much as 15 km, and would be expected to give a large change in Z.

Within 1 h of sunrise or sunset, particularly in summer, the observed value of $|\,_{\parallel}R_{\perp}|$ undergoes marked changes. For nearly vertical incidence in summer, the change is by a factor of 3 or 4. With the exponential model this change could only be associated with a large change of Z (see figure 9), and therefore of reflexion height. There is, however, no appreciable observed change of apparent height of reflexion for nearly vertical incidence, so that the 'exponential' model is again inadequate to account for the observations.

(*e*) *Summarizing remarks on the 'exponential' model of the ionosphere*

It is clear from the preceding sections that the 'exponential' model of the ionosphere with vertical magnetic field will explain only the broad qualitative features of the observations at 16 kc/s, and fails when a more detailed quantitative correlation is attempted. It is therefore desirable to choose a different model.

An obvious extension would be to repeat the calculations allowing for the obliquity of the earth's magnetic field. Another possibility was to use a different law for the monotonic increase of electron density with height. A few calculations were made for a model ionosphere in which the earth's magnetic field was vertical, and the electron density varied as in the lower part of a 'Chapman' layer. They were not, however, numerous enough for detailed analysis, and because of the marked effect of the obliquity of the earth's magnetic field (see §4 (*b*)) further calculations of this kind have been postponed until the second method of paper I is available with oblique field. Instead, subsequent calculations were devoted to a study of a model ionosphere, in which the electron density was not a monotonic function of height, but included a D-layer. These calculations are described in the following sections.

7. Calculations with constant Z and vertical magnetic field for ionosphere with a 'D-layer'

The need for postulating a D-layer to explain the results of observations at very low frequencies (mainly 16 kc/s) has been stressed by several authors (Bracewell & Bain 1952; Bracewell 1952; Bain 1953). Workers at the Pennsylvania State University, U.S.A., have proposed a model of the ionosphere which includes a D-layer and which, according to

their very detailed calculations, explains the observations made for vertical incidence at a frequency of 150 kc/s (see, for example, Kelso, Nearhoof, Nertney & Waynick 1951; Nertney 1953). They have also examined the properties of this model for vertical incidence at other frequencies, and find that they are consistent with the observations. It was therefore considered important to investigate the general properties of a model ionosphere with a D-layer for very low frequencies, and, in particular, to include a study of the properties at oblique incidence. The calculations described in the following sections were all made for a frequency of 16 kc/s, and for the fixed value $Z = 30$, and the earth's magnetic field was assumed to be vertical.

(*a*) *Choice of the form of the D-layer*

In view of the great success of the models adopted by workers at the Pennsylvania State University, in explaining the observations at 150 kc/s, it was desirable to examine the properties of the same models at 16 kc/s. This would have led, however, to some difficulties in programming the calculations. Moreover, these were made only with a vertical magnetic field for which the results are known to be appreciably different from those obtained with an oblique field (see §4 (*b*)). The calculations could therefore be made only with the object of establishing general properties of a D-layer, and not for the determination of an exact model. The somewhat simplified model described below was therefore adopted.

Figure 11 shows how the electron density N varies with height z, in a typical model ionosphere as used for the calculations. In the upper part of the curve N varies according to the Chapman law, and this part may be thought of as the bottom of a 'Chapman E-layer', calculated for an isothermal atmosphere of scale height 10 km with a penetration frequency of 4·4 Mc/s. The D-layer forms the lower part of the full curve, and is given by the Gaussian law

$$X = X_m \exp\{-(z-z_m)^2/2w^2\}. \tag{4}$$

The maximum of the D-layer occurs at the height $z = z_m$, which was chosen to be at 40 km below the maximum of the Chapman E-layer, since this is the value adopted for midday by Nertney (1951). The maximum value X_m of X in the D-layer for a frequency of 16 kc/s was chosen to be 284, to correspond to an electron density of 1000 cm^{-3}, the value used by Nertney. The value of w in (4) was chosen so that the width of the Gaussian curve at half its maximum value was about 5 km, which made the total electron content of the D-layer roughly the same as in Nertney's models. The term 'Gaussian D-layer of strength 1' will in future be used for a D-layer to this specification, and the term 'Gaussian D-layer of strength S' will mean a similar layer with an electron density S times that for the layer of strength 1.

Figure 11 also shows (dashed curve) one of the forms of D-layer used by Nertney. This is a Chapman region for an isothermal atmosphere with a scale height of 1 km. A few calculations were made for this model, and the results are mentioned in later sections. The gradient of electron density is, however, very great for the lower part of this model, and the size of the step used for the integrations may have been too large, so that truncation errors were introduced. The results should therefore be treated with reserve. Most of the calculations were made for Gaussian layers of strength 1 or less, with the fixed Chapman

E-layer above it, and the gradients of electron density were known to be small enough to give reliable results.

One of the requirements that a *D*-layer must fulfil is that it must not give excessive absorption at high frequencies. Table 2 shows the factor by which the amplitude of a signal of frequency 1 Mc/s would be reduced by a single and a double passage through Gaussian *D*-layers of various strengths. The values are calculated approximately, neglecting the effect of the earth's magnetic field. From these figures it is clear that a Gaussian

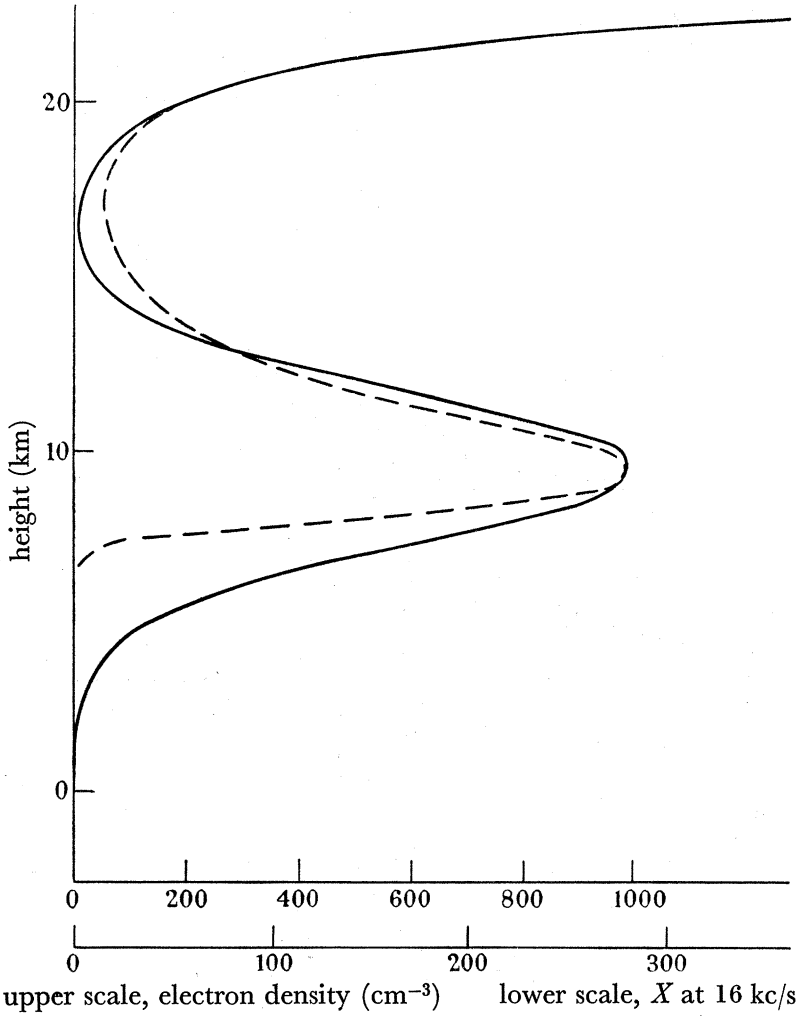

FIGURE 11. Variation of electron density with height for model ionosphere with Gaussian *D*-layer of strength 1 (full curve). The dashed curve shows one of the Chapman type *D*-layer models as used by Nertney.

TABLE 2. ABSORPTION OF 1 MC/S SIGNALS BY GAUSSIAN *D*-LAYERS ($Z = 30$)

strength of Gaussian *D*-layer	critical frequency (kc/s)	ratio of signal amplitudes	
		single passage	double passage
1	270	0·21	0·04
$\frac{1}{2}$	191	0·41	0·17
$\frac{1}{5}$	121	0·73	0·54
$\frac{1}{10}$	85	0·86	0·73
$\frac{1}{25}$	54	0·94	0·88
$\frac{1}{50}$	38	0·97	0·94

D-layer of strength 1 produces fairly great absorption at 1 Mc/s. This strength was therefore taken as the upper limit for the models of the ionosphere which could be accepted.

(*b*) *Variation of amplitude of reflexion coefficient with angle of incidence*

Some typical curves to show how the reflexion coefficient $|{}_{\parallel}R_{\parallel}|$ varied with angle of incidence are given in figure 12. One curve in the top diagram is for a Chapman layer alone without a D-layer below it. Two others are for Gaussian D-layers alone, of strengths 1 and $\frac{1}{10}$. In calculating these two curves, the integrations were started in a region of free space above the D-layer, where the 'initial solutions' (see paper I) had to be calculated

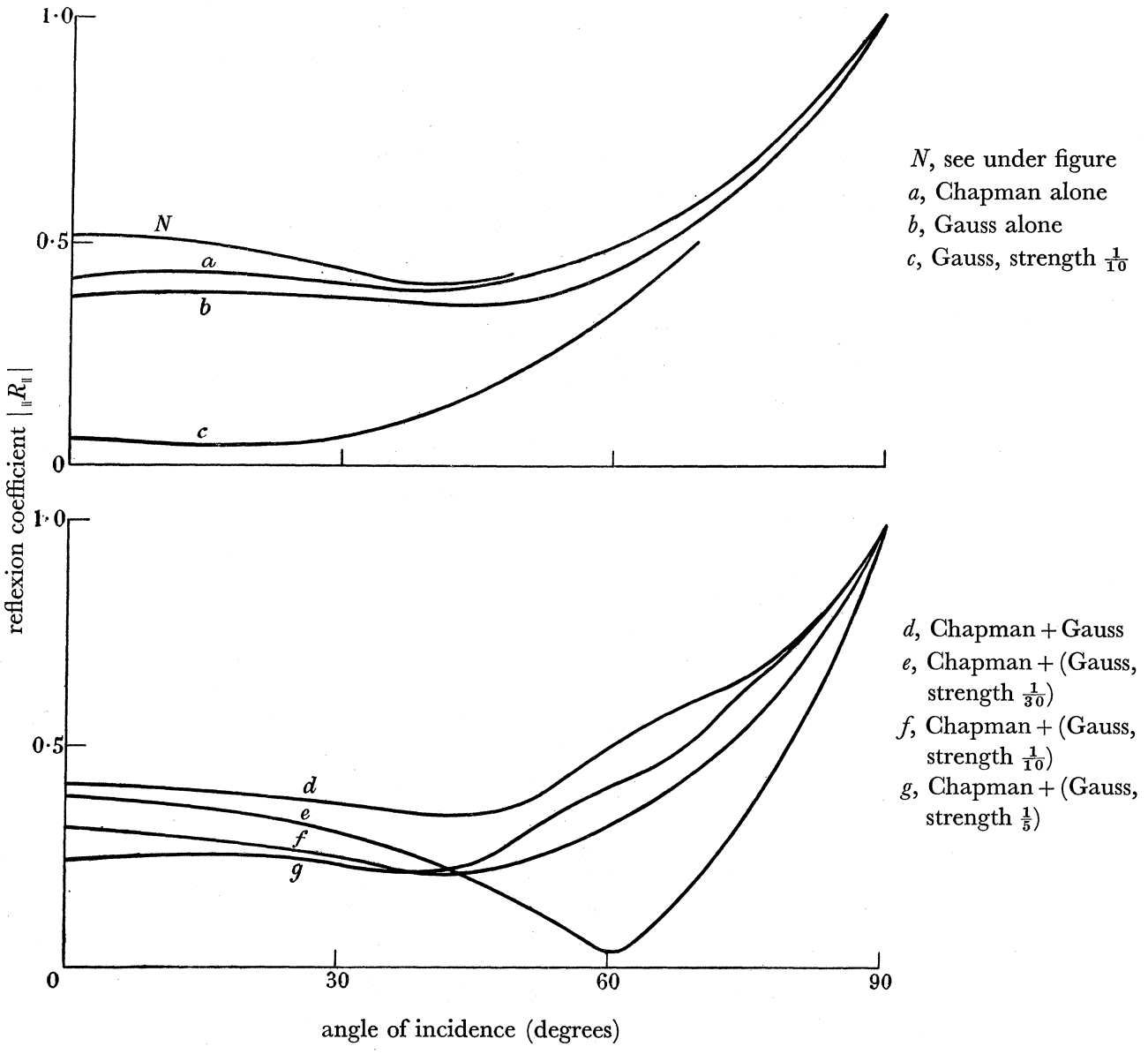

FIGURE 12. Variation of reflexion coefficient $|{}_{\parallel}R_{\parallel}|$ with angle of incidence. Vertical magnetic field. $Z = 30$. The curve marked 'N' is for a vertical magnetic field and for a Chapman E-layer with Nertney's model D-layer below it (dashed curve of figure 11).

separately for each value of the angle of incidence. For this purpose a simple modification of the program described in paper I was used. The remaining curve in the top diagram is for Nertney's model ionosphere as shown by the dashed curve in figure 11. It should be remembered, however, that the curve of figure 12 is for vertical magnetic field and fixed Z, whereas Nertney's calculations were made for an oblique field and for varying Z. The bottom four curves of figure 12 are for a Chapman E-layer with Gaussian D-layers of various strengths below it. Figure 13 shows how $|{}_{\parallel}R_{\perp}|$ varies with angle of incidence for the same models of the ionosphere as in figure 12.

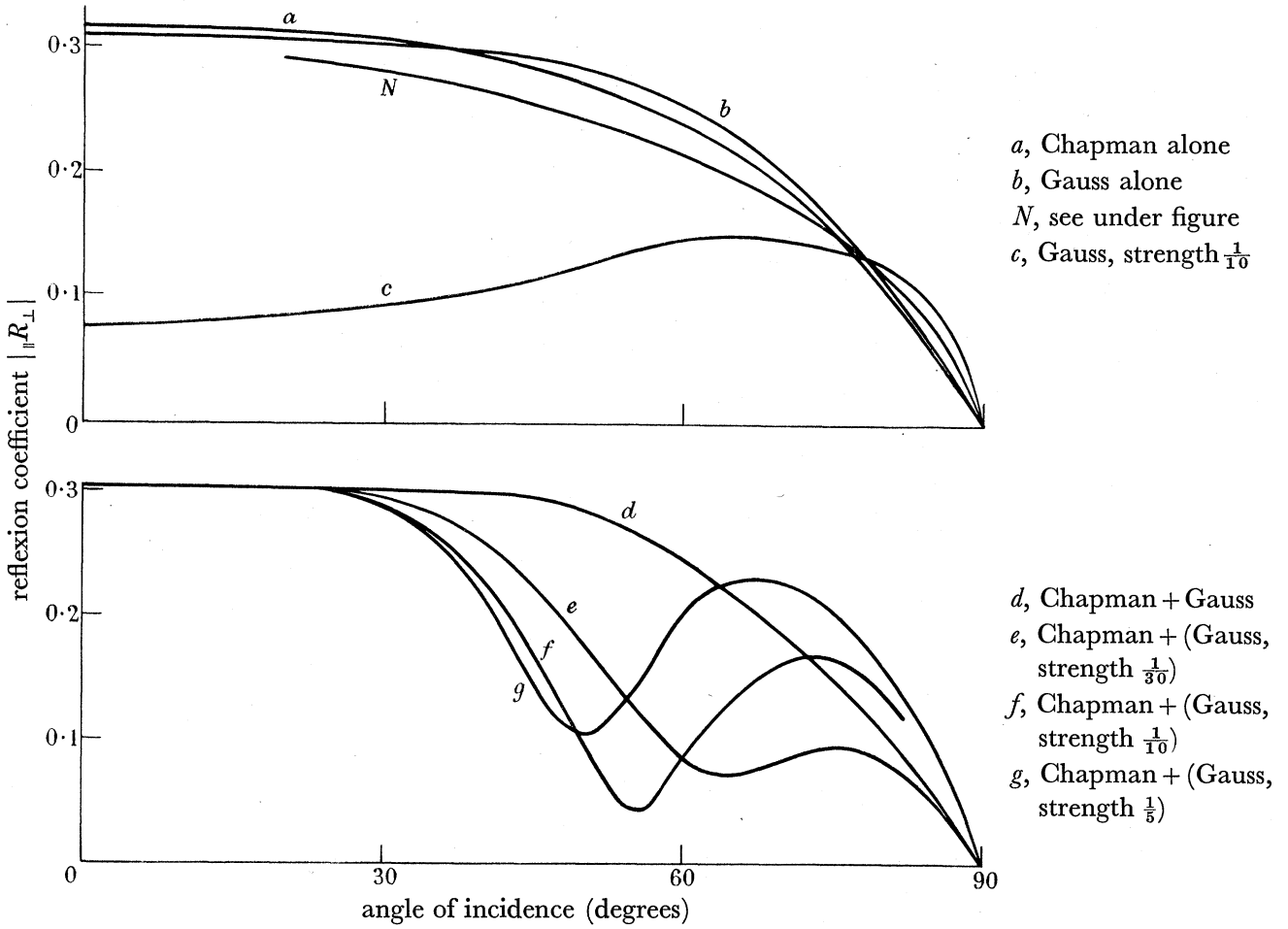

FIGURE 13. Variation of reflexion coefficient $|{}_{\parallel}R_{\perp}|$ with angle of incidence. Vertical magnetic field. $Z = 30$. The curve marked 'N' is for a vertical magnetic field and for a Chapman E-layer with Nertney's model D-layer below it (dashed curve of figure 11).

Figures 12 and 13 show that there is very little difference between the reflecting properties of a Chapman layer and a Gaussian D-layer of strength 1. This might be expected from the results of §6 (a), where it was shown that reflexion probably occurs below the level where $X = 80$. In the lower part of a Gaussian D-layer of strength 1, X increases monotonically up to the value of 284, so that it might be expected to behave in a roughly similar way to an 'exponential' ionosphere, and the same applies to the lower part of the Chapman region. For the Gaussian D-layer of strength $\frac{1}{10}$, however, X increases up to only 28·4, so that some energy might be expected to penetrate the layer with a consequent

decrease of the reflexion coefficients. This decrease is clearly shown in the top diagrams of figures 12 and 13.

For model ionospheres with both D- and E-layers, reflexion may occur partly from one layer and partly from the other. It is thus possible for interference between the two reflexions to take place. The curve in figure 12 for a Chapman E-layer accompanied by a Gaussian D-layer of strength $\frac{1}{30}$ shows that destructive interference is nearly complete, in this case, for an angle of incidence of about 60°. It can, in fact, be shown (see §7 (f))

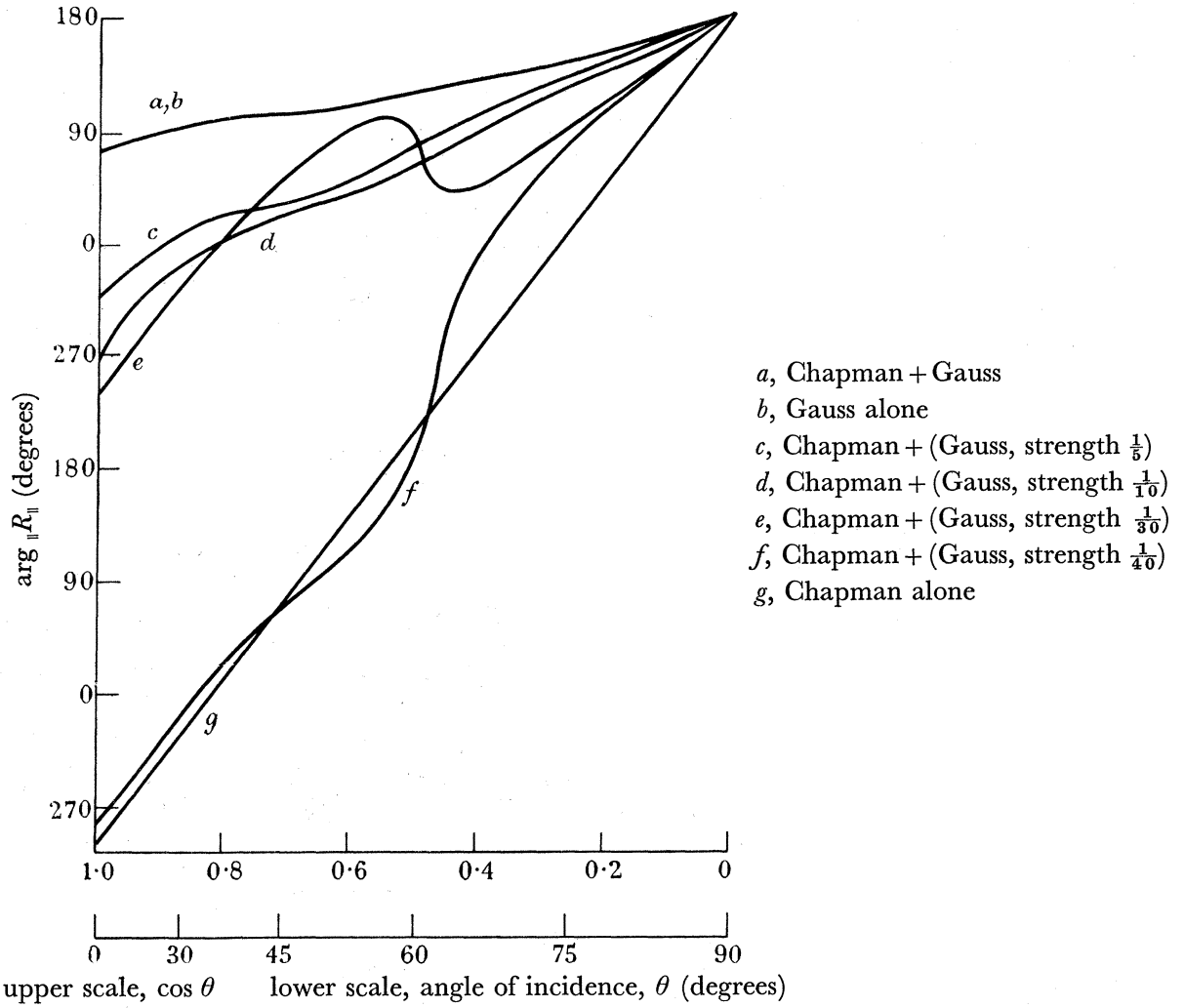

FIGURE 14. Variation of arg $_{\parallel}R_{\parallel}$ with cosine of angle of incidence. The reference level is at 0 km on the scale of figure 11.

that there must be some strength of the D-layer and some angle of incidence for which $|_{\parallel}R_{\parallel}|$ is exactly zero. The same is true for $|_{\parallel}R_{\perp}|$ but with a different strength of D-layer, and a different value of the angle of incidence, as is apparent from the lower diagram of figure 13.

(c) *Phase of the reflexion coefficient and the apparent height of reflexion*

For ionosphere models with a D-layer, it is of interest to find the apparent height of reflexion, as was done in §6 (a) for the exponential model (for the definition of 'apparent

height of reflexion' see §3). For this purpose the value of arg $_{\parallel}R_{\parallel}$ is plotted against cos θ in figure 14, for various models. The curve for the Chapman region alone is seen to be fairly straight and gives an apparent height of reflexion, for all angles of incidence, of about 17 km on the scale of figure 11. The value of X at this level is about 1·5.

The curves for a Chapman layer with a Gaussian D-layer of strength 1 below it, and for a Gaussian layer of strength 1 alone, are indistinguishable, which confirms the conclusion of the last section that reflexion occurs almost entirely in the lower part of the D-layer. The curve in this case also is practically straight, and gives an apparent height of reflexion, for all angles of incidence, of about 3 km on the scale of figure 11. The value of X at this level is about 2·6.

For D-layers of other strengths the effective height of reflexion is different for different ranges of angles of incidence. For a D-layer of strength $\frac{1}{30}$, for small angles of incidence, the curve is nearly straight and parallel to that for the Chapman region alone, showing that the apparent height of reflexion is near the bottom of the Chapman region. There is, however, a rather abrupt change near 60°, and for still more oblique incidence the curve is again nearly straight, but with a smaller slope corresponding to an apparent reflexion level near the maximum of the D-layer. The abrupt change is clearly associated with the minimum in $|_{\parallel}R_{\parallel}|$, shown in figure 12. The curve for a D-layer of strength $\frac{1}{40}$ is similar, except that the abrupt change is in the opposite sense. It is shown in §7 (f) that there must be a D-layer of strength between $\frac{1}{30}$ and $\frac{1}{40}$, for which $|_{\parallel}R_{\parallel}|$ has a zero at some angle of incidence near 60°.

(*d*) *Polarization of the reflected wave*

The curves in figure 15 show how arg $_{\parallel}R_{\perp}$ − arg $_{\parallel}R_{\parallel}$ varies with angle of incidence. This quantity is the phase difference between the normal and abnormal components of the reflected wave when the incident wave is linearly polarized in the plane of incidence. From this and the quantities $|_{\parallel}R_{\parallel}|$ and $|_{\parallel}R_{\perp}|$ the polarization of the reflected wave may be deduced. Figure 15 is plotted for the same models of the ionosphere as in figures 12 and 13. These figures show that for near-vertical incidence the polarization of the reflected wave is roughly circular with a left-handed sense, as it was for the exponential models (§6 (b)). For the models having a Chapman layer alone, a Gaussian layer of strength 1, or a combination of the two (top diagram, figure 15), the polarization changes to nearly linear at large angles of incidence in a similar way to the change that occurs with the exponential models. For models which include Gaussian layers of smaller strengths, however, there are more abrupt changes of polarization caused by the minima in $|_{\parallel}R_{\parallel}|$ and $|_{\parallel}R_{\perp}|$ and by rapid changes in arg $_{\parallel}R_{\perp}$ − arg $_{\parallel}R_{\parallel}$, with angle of incidence. No observations seem to have been reported in which a change of the angle of incidence is accompanied by such a marked change of polarization.

(*e*) *D-layers of variable strength*

It has been suggested (Bracewell & Bain 1952) that the D-layer in the ionosphere is formed at a time near sunrise when the sun's rays first reach the level of the layer, and that it disappears again near sunset. It is therefore of interest to investigate the changes that would occur as the strength of the D-layer changes, and to compare the results with

observations made near sunrise and sunset. For this purpose the curves of figures 16 and 17 have been plotted to show how $|{}_{\parallel}R_{\parallel}|$ and $|{}_{\parallel}R_{\perp}|$ respectively vary with the strength of the Gaussian D-layer, for various angles of incidence. The abscissae in these figures are proportional to $S^{\frac{1}{3}}$, where S is the strength of the Gaussian D-layer. This scale was chosen to display the results to best advantage.

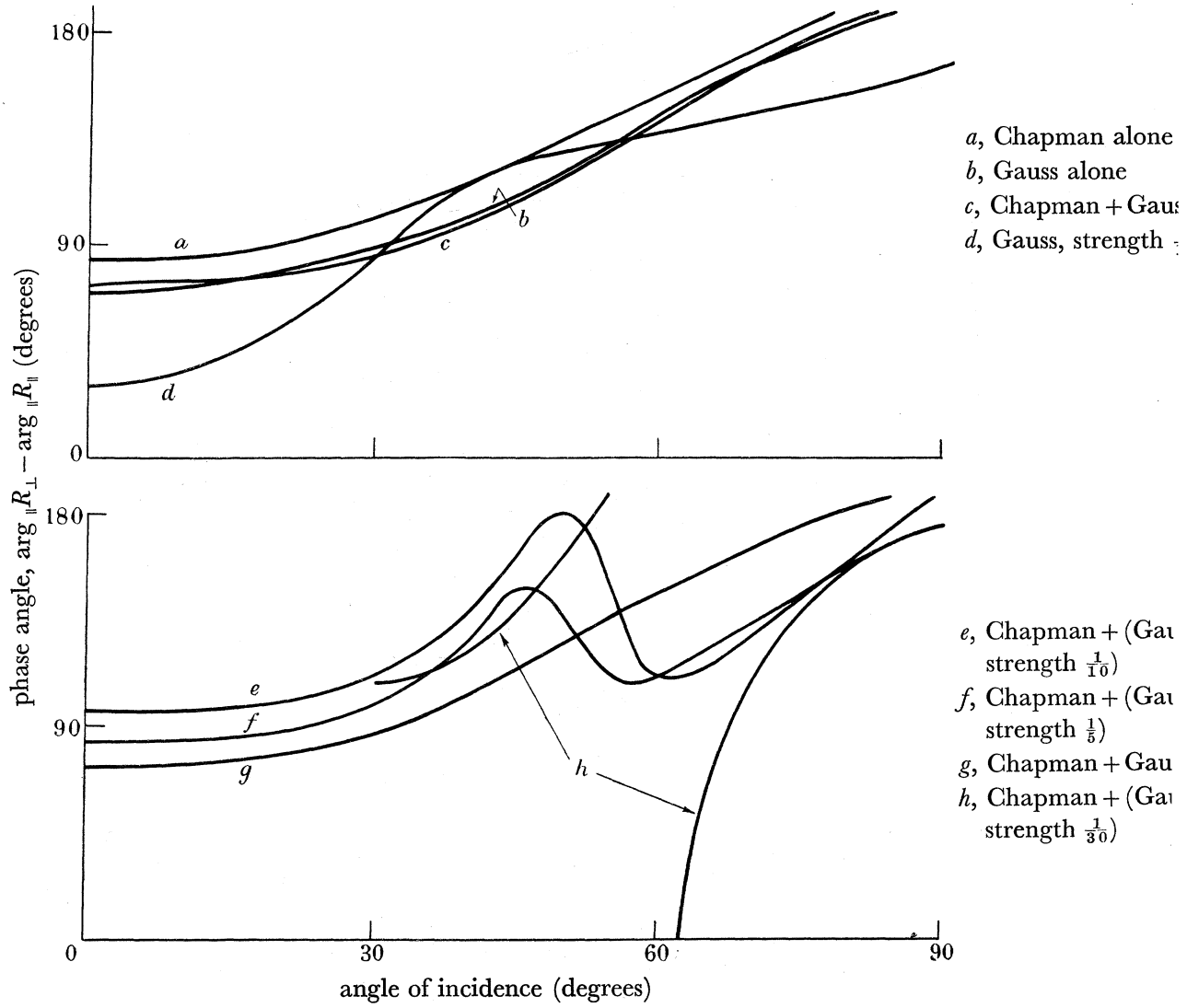

FIGURE 15. Phase difference between ${}_{\parallel}R_{\perp}$ and ${}_{\parallel}R_{\parallel}$, as a function of angle of incidence.

The striking feature of the curves of figure 16 is the minimum which occurs for angles of incidence near 60°, when the strength of the D-layer increases. Now for radio signals transmitted over distances greater than 400 km, the angle of incidence of a ray making a single reflexion at the ionosphere is greater than 60°, but cannot exceed about 80° because of the earth's curvature. Hence the signal received on a vertical aerial (assuming that the transmitting aerial is also vertical) would be expected to pass through a minimum if a D-layer were formed at about 40 km below the main reflecting E-layer.

Some preliminary calculations for a frequency of 71·1 kc/s and the same model of the ionosphere as in figures 16 and 17, show that for this frequency also there is a marked

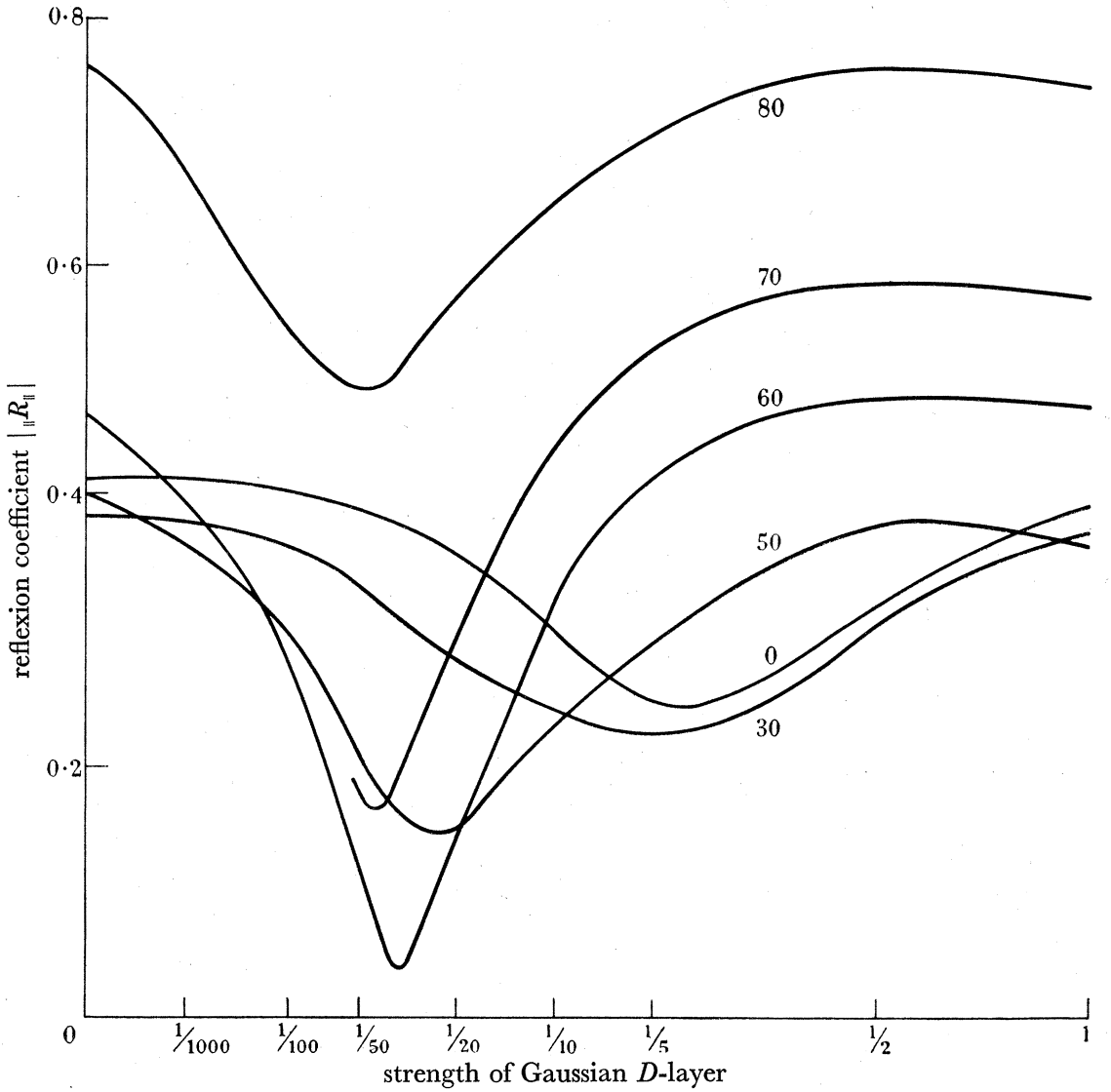

FIGURE 16. Variation of $|_{\parallel}R_{\parallel}|$ with strength of Gaussian D-layer, for various angles of incidence θ (degrees). Maximum of D-layer is 40 km below maximum of Chapman E-layer. Vertical magnetic field. $Z = 30$.

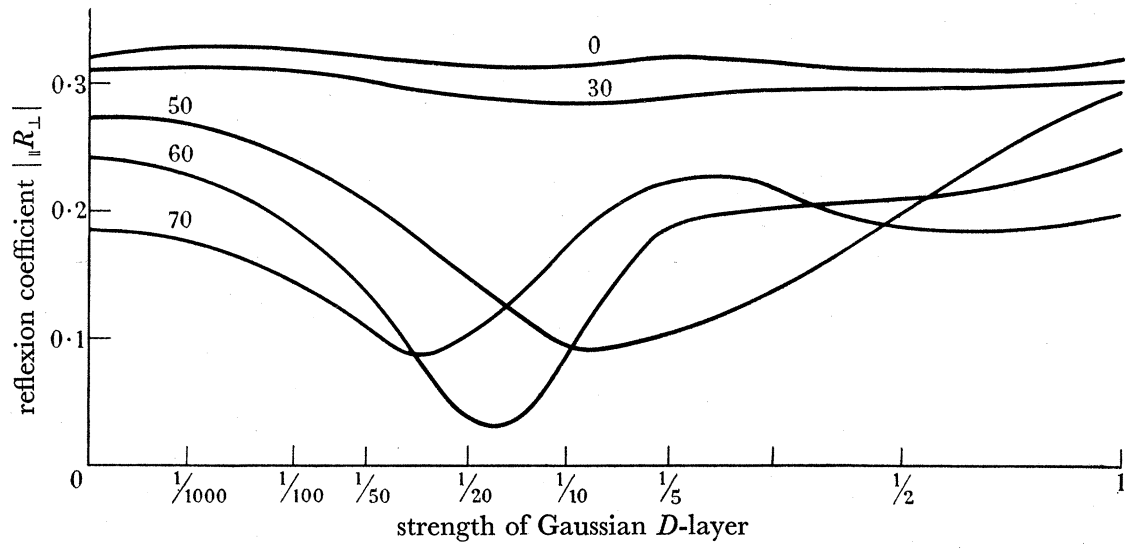

FIGURE 17. Variation of $|_{\parallel}R_{\perp}|$ with strength of Gaussian D-layer, for various angles of incidence θ (degrees). Maximum of D-layer is 40 km below maximum of Chapman E-layer. Vertical magnetic field. $Z = 30$.

minimum in $|{}_{\parallel}R_{\parallel}|$ for an angle of incidence near 60° and for a Gaussian D-layer of strength about $\frac{1}{10}$.

Many measurements show that for low- and very low-frequency radio waves transmitted over distances between about 400 and 2000 km there is a marked minimum near sunrise and another minimum, often less pronounced, near sunset (see, for example, Bain, Bracewell, Straker & Westcott (1952), and the references given there). This applies in particular to waves of frequency 16 kc/s from the sender GBR, Rugby, received at Aberdeen 540 km away. The calculations therefore give support to the suggestion (e.g. Bracewell & Bain 1952) that a D-layer is formed near sunrise and disappears again near sunset. Figure 17 shows that the calculations also give a minimum in $|{}_{\parallel}R_{\perp}|$. The observations are not detailed enough to say whether such a minimum is found in practice, since the measurement of $|{}_{\parallel}R_{\perp}|$ for very oblique incidence is difficult.

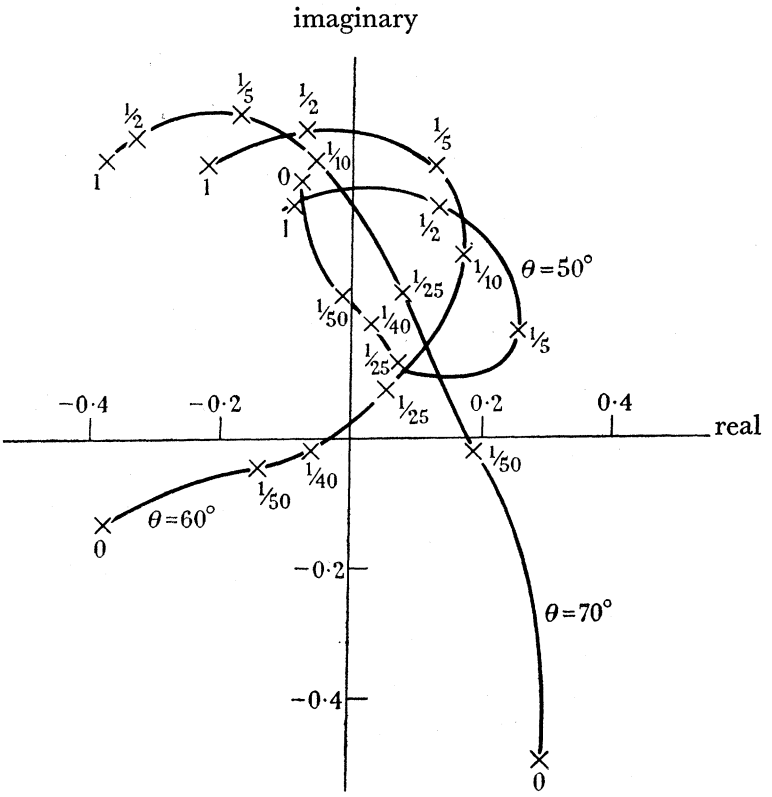

FIGURE 18. Representation of ${}_{\parallel}R_{\parallel}$ in the complex plane. The reference level for arg ${}_{\parallel}R_{\parallel}$ is at 0 km in figure 11. The numbers beside the points give the strength of the Gaussian D-layer.

(*f*) *Polar diagrams for* ${}_{\parallel}R_{\parallel}$

It is instructive to display the results of figure 16 in a slightly different way, so that values of arg ${}_{\parallel}R_{\parallel}$ can also be shown. In figure 18 the values of the complex quantity ${}_{\parallel}R_{\parallel}$ are plotted in the complex plane, so that for any point the radius vector from the origin is of length $|{}_{\parallel}R_{\parallel}|$ and makes an angle arg ${}_{\parallel}R_{\parallel}$ from a reference line. Each curve is plotted for a fixed angle of incidence, and the points on it are for Gaussian D-layers of different strengths, as indicated in the figure.

It is clear that there must be a continuous transition from one curve in figure 18 to the next, as the angle of incidence θ increases. Thus the curve for $\theta = 50°$ is closed, but would open out as θ increased so as to change to the 60° curve. A further slight increase in θ would make the curve cross the origin in order to pass continuously to the curve for $\theta = 70°$. Hence there must be a value of θ near 61° for which the curve passes through the origin, and for this curve $|{}_{\parallel}R_{\parallel}|$ is zero for a Gaussian D-layer of strength about $\frac{1}{30}$. This establishes the result stated near the end of §7 (b).

8. Conclusion

The calculations described in the preceding sections were nearly all made for a frequency of 16 kc/s, and for a fixed value of collision frequency and a vertical superimposed magnetic field. They suggest a possible basis for a number of salient features in the observations at 16 kc/s, but fall far short of indicating a model of the ionosphere which can be used to explain most of the observed behaviour.

The assumption of a vertical magnetic field constitutes a particularly severe limitation on the detailed correlation of the results with observations. For this reason the calculations for 16 kc/s have now been suspended. Future work is developing along two separate lines: (a) calculations with vertical magnetic field for frequencies other than 16 kc/s, (b) calculations with an oblique magnetic field. Work under (a) is now in progress, and some preliminary results have been obtained for a frequency of 71·1 kc/s. For calculations in category (b) the second method of calculation described in paper I is being developed. This method is already working well for the calculations in category (a), and should greatly speed up the more complicated calculations with an oblique field.

I am indebted to the director and staff of the University Mathematical Laboratory, Cambridge, for permission to use the EDSAC.

References

Appleton, E. V. 1932 *J. Instn Elect. Engrs*, **71**, 642.
Bain, W. C. 1953 *J. Atmos. Terr. Phys.* **3**, 141.
Bain, W. C., Bracewell, R. N., Straker, T. W. & Westcott, C. H. 1952 *Proc. Instn Elect. Engrs*, **99**, IV, 250.
Best, J. E., Ratcliffe, J. A. & Wilkes, M. V. 1936 *Proc. Roy. Soc.* A, **156**, 614.
Bracewell, R. N. 1952 *J. Atmos. Terr. Phys.* **2**, 226.
Bracewell, R. N. & Bain, W. C. 1952 *J. Atmos. Terr. Phys.* **2**, 216.
Bracewell, R. N., Budden, K. G., Ratcliffe, J. A., Straker, T. W. & Weekes, K. 1951 *Proc. Instn Elect. Engrs*, **98**, III, 221.
Budden, K. G. 1951 *Phil. Mag.* **42**, 833.
Budden, K. G. 1953 *Phil. Mag.* **44**, 504.
Budden, K. G. 1954 *Proc. Camb. Phil. Soc.* **50**, 604.
Budden, K. G. 1955 *Proc. Roy. Soc.* A, **227**, 516 (paper I).
Budden, K. G., Ratcliffe, J. A. & Wilkes, M. V. 1939 *Proc. Roy. Soc.* A, **171**, 188.
Chapman, S. 1931 *Proc. Phys. Soc. Lond.* **43**, 26, 484.
Gibbons, J. J. & Nertney, R. J. 1951 *J. Geophys. Res.* **56**, 355.
Heading, J. & Whipple, R. T. P. 1952 *Phil. Trans.* A, **244**, 469.

PHILOSOPHICAL TRANSACTIONS OF THE ROYAL SOCIETY A MATHEMATICAL, PHYSICAL & ENGINEERING SCIENCES

Kelso, J. M., Nearhoof, H. J., Nertney, R. J. & Waynick, A. H. 1951 *Ann. Géophys.* **7**, 215.
Nertney, R. J. 1951 *Tech. Rep. Pa St. Coll.* no. 20.
Nertney, R. J. 1953 *J. Atmos. Terr. Phys.* **3**, 92.
Nicolet, M. 1953 *J. Atmos. Terr. Phys.* **3**, 200.
Pedersen, P. O. 1927 *The propagation of radio waves.* Copenhagen: Danmarks Naturvidenskabelige Samfund.
Tremellen, K. W. 1950 *Marconi Rev.* **13**, 153.
Weekes, K. 1950 *Proc. Instn Elect. Engrs*, **97**, III, 100.

PHILOSOPHICAL TRANSACTIONS OF THE ROYAL SOCIETY A MATHEMATICAL, PHYSICAL & ENGINEERING SCIENCES